

# Entanglement Driven Phase Transitions in Spin-Orbital Models

Wen-Long You,<sup>1,2</sup> Andrzej M. Oleś,<sup>1,3</sup> and Peter Horsch<sup>1</sup>

<sup>1</sup>Max-Planck-Institut für Festkörperforschung, Heisenbergstrasse 1, D-70569 Stuttgart, Germany

<sup>2</sup>School of Physical Science and Technology, Soochow University, Suzhou, Jiangsu 215006, People's Republic of China

<sup>3</sup>Marian Smoluchowski Institute of Physics, Jagiellonian University, prof. S. Łojasiewicza 11, PL-30348 Kraków, Poland

(Dated: September 26, 2018)

To demonstrate the role played by the von Neumann entropy spectra in phase transitions we investigate the one-dimensional spin-orbital  $SU(2) \otimes XXZ$  model with negative exchange parameter and anisotropic  $XXZ$  orbital interactions. When the orbital interactions are Ising-like a novel phase with spin-singlet dimer correlations and large spin-orbital entanglement entropy is found, while all the other phases are disentangled. For anisotropic  $XXZ$  orbital interactions the antiferro-spin/alternating-orbital phase becomes also entangled and inherits dimer correlations by proximity to the dimer phase. This phase provides a unique example of coupled order parameters which change the character of the phase transition from first-order to continuous. Thus we demonstrate that the von Neumann entropy spectral function is a valuable tool to identify the change of character of elementary excitations and of ground state degeneracies at quantum phase transitions.

PACS numbers: 75.25.Dk, 03.67.Mn, 05.30.Rt, 75.10.Jm

In the Mott-insulating limit of a transition metal oxide the low-energy physics can be described by Kugel-Khomskii-type models [1], where both the spin and the orbital degrees of freedom are quantum dynamic variables. Following the microscopic derivation from the multiorbital Hubbard model, the generic structure of spin-orbital superexchange takes the form of a generalized Heisenberg model [2, 3],

$$H = \sum_{\langle ij \rangle \parallel \gamma} \left\{ J_{ij}^{(\gamma)} (\vec{T}_i, \vec{T}_j) \vec{S}_i \cdot \vec{S}_j + K_{ij}^{(\gamma)} (\vec{T}_i, \vec{T}_j) \right\}. \quad (1)$$

Here the parameters that determine the spin- $S$  Heisenberg interactions stem from  $J_{ij}^{(\gamma)}$  and  $K_{ij}^{(\gamma)}$  — they depend on the bond direction and are controlled by the orbital degree of freedom which is described by pseudospin operators  $\{\vec{T}_i\}$ . That is, these parameters are not necessarily fixed by rigid orbital order [4, 5], but quantum fluctuations of orbital occupation [6, 7] may strongly influence them and lead to spin-orbital entanglement (SOE) [8, 9]. As a consequence, amplitudes and even the signs of the effective exchange can fluctuate. Such entangled spin-orbital degrees of freedom can form new states of matter, as for instance the orbital-Peierls state observed at finite temperature in  $YVO_3$  [10, 11]. It is challenging to ask which measure of SOE would be the most appropriate one to investigate quantum phase transitions in such systems.

The subject is rather general and it has become clear that entanglement and other concepts from quantum information provide a useful perspective for the understanding of electronic matter [12–16]. Other examples of entangled systems are: topologically nontrivial states [17], relativistic Mott insulators with  $5d$  ions [18], ultracold alkaline-earth atoms [19], and skyrmion lattices in the chiral metal  $MnSi$  [20].

One well-known characterization of a quantum system is the entanglement entropy (EE) determined by bipartitioning a system into  $A$  and  $B$  subsystems. This subdivision can refer for example to space [12, 21], momentum [21, 22], or different degrees of freedom [23]. A standard measure is the von Neumann entropy (vNE),  $S_{vN}^0 \equiv -\text{Tr}_A\{\rho_A^0 \log_2 \rho_A^0\}$ , for the

ground state  $|\Psi_0\rangle$  which is obtained by integrating the density matrix,  $\rho_A^0 = \text{Tr}_B|\Psi_0\rangle\langle\Psi_0|$ , over subsystem  $B$ . An important measure is the entanglement spectrum (ES) introduced by Li and Haldane [24], which has been explored for gapped one-dimensional (1D) spin systems [25, 26], quantum Heisenberg ladders [27], topological insulators [28], bilayers and spin-orbital systems [21]. The ES is a *property of the ground state* and basically represents the eigenvalues  $p_i$  of  $\rho_A^0$  obtained by bipartitioning of the system. Interestingly a correspondence of the ES and the tower of excitations relevant for  $SU(2)$  symmetry breaking was pointed out recently [29]. It was also noted that the ES can exhibit singular changes, although the system remains in the same phase [30]. Thus the ES appears to have less universal character than initially assumed [31].

In this Letter we explore a different entanglement measure, namely the vNE spectrum which monitors the ground and *excited states* of a spin-orbital system as in Eq. (1). We consider the entanglement obtained from the bipartition into spin and orbital degrees of freedom [23]. Here the vNE is obtained from the density matrix,  $\rho_s^{(n)} = \text{Tr}_o|\Psi_n\rangle\langle\Psi_n|$ , by taking the trace over the orbital degrees of freedom ( $\text{Tr}_o$ ) for each eigenstate  $|\Psi_n\rangle$ . We show below that the vNE spectrum,

$$S_{vN}(\omega) = - \sum_n \text{Tr}_s\{\rho_s^{(n)} \log_2 \rho_s^{(n)}\} \delta\{\omega - \omega_n\}, \quad (2)$$

reflects the changes of SOE entropy for the different states at phase transitions. The excitation energies,  $\omega_n = E_n - E_0$ , of eigenstates  $|\Psi_n\rangle$  are measured with respect to the ground state energy  $E_0$ . It has already been shown that the vNE spectra uncover a surprisingly large variation of entanglement of elementary excitations [23]. Also certain spectral functions have been proposed, that can be determined by resonant inelastic x-ray scattering [32], and provide a measure of the vNE spectral function. Here we generalize this function to arbitrary excitations  $|\Psi_n\rangle$ , i.e., beyond elementary excitations. We demonstrate that focusing on general excited states opens up a new perspective that sheds light on quantum phase transitions and

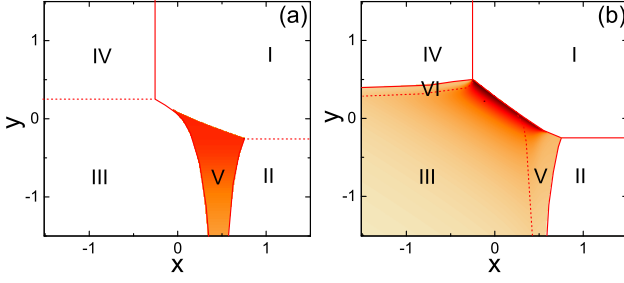


FIG. 1. (color online). Phase diagrams of the spin-orbital model [Eq. (3)] obtained by two methods, fidelity susceptibility or an exact diagonalization of an  $L = 8$  site model, for: (a)  $\Delta = 0$ , and (b)  $\Delta = 0.5$  [48]. The spin-orbital correlations in phases I-IV correspond to FS/FO, AS/FO, AS/AO, FS/AO order (see text). At  $\Delta = 0$  only the ground state of a novel phase V has finite EE,  $S_{\text{vN}}^0 > 0$  (shaded), whereas at  $\Delta > 0$  the EE in phases III and VI is also finite.

the entanglement in spin-orbital systems.

Central for our theoretical discussion of spin-orbital physics are  $t_{2g}$  electron systems in which orbital quantum fluctuations are enhanced by intrinsic lowering the dimensionality [33]. Examples of strongly entangled 1D  $t_{2g}$  spin-orbital systems due to dimensional reduction occur in  $\text{LaTiO}_3$  [6],  $\text{LaVO}_3$  and  $\text{YVO}_3$  [7], where the latter two involve  $\{yz, zx\}$  orbitals along the  $c$  cubic axis; as well as  $p_x$  and  $p_y$  orbital systems in 1D fermionic optical lattices [34, 35]. This motivates us to consider the 1D spin-orbital model for  $S = 1/2$  spins and  $T = 1/2$  orbital  $XXZ$  interaction, with  $|+\rangle$  and  $|-\rangle$  orbital ( $yz$  and  $zx$ ) states and free coupling parameters  $\{x, y\}$ ,

$$\mathcal{H}(x, y, \Delta) = J \sum_j \left( \vec{S}_j \cdot \vec{S}_{j+1} + x \right) \left( [\vec{T}_j \cdot \vec{T}_{j+1}]_{\Delta} + y \right), \quad (3)$$

where  $[\vec{T}_j \cdot \vec{T}_{j+1}]_{\Delta} \equiv \Delta (T_j^x T_{j+1}^x + T_j^y T_{j+1}^y) + T_j^z T_{j+1}^z$ . At  $x = y = 1/4$  and  $\Delta = 1$  the model has  $\text{SU}(4)$  symmetry. Hund's coupling does not only modify  $x$  and  $y$  but also leads to the  $XXZ$  anisotropy ( $\Delta < 1$ ), a typical feature of the orbital sector in real materials [3, 33]. The antiferromagnetic (AF) model ( $J = 1$ ) is Bethe-Ansatz integrable at the  $\text{SU}(4)$  symmetric point [36], its phase diagram is well established by numerical studies [37, 38], including two phases with dimer correlations [39]. Some of its ground states could be even determined exactly at selected  $(x, y, \Delta)$  points [40–44].

Here we are interested in the complementary and less explored model with negative (ferromagnetic) coupling ( $J = -1$ ), possibly realized in multi-well optical lattices [45], which has been studied so far only for  $\text{SU}(2)$  orbital interaction ( $\Delta = 1$ ) [23]. This model is physically distinct from the  $J = 1$  model, except for the not yet investigated Ising ( $\Delta = 0$ ) limit where the two models can be mapped onto each other. The phase diagrams for  $J = -1$  (Fig. 1) determined using the fidelity susceptibility [46] display the simple rule that the vNE (2) vanishes for exact ground states of rings of length  $L$  which can be written as a product of spin ( $|\psi_s\rangle$ ) and orbital ( $|\psi_o\rangle$ ) part,  $|\Psi_0\rangle = |\psi_s\rangle \otimes |\psi_o\rangle$ . In the case  $\Delta = 0$  all trivial combinations of ferro (F) and antiferro (A) spin/orbital

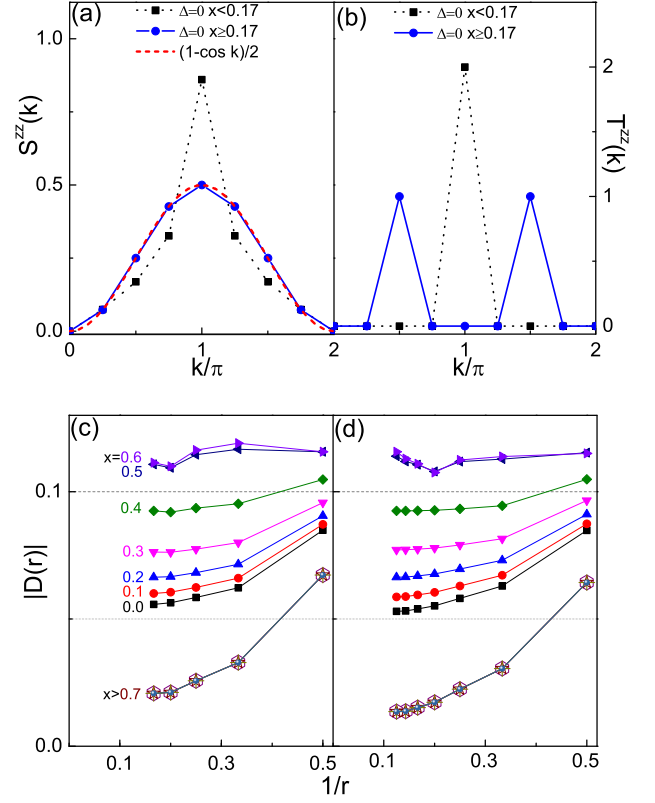


FIG. 2. (color online). Top— Spin [ $S^{zz}(k)$ ] and orbital [ $T^{zz}(k)$ ] structure factors (4) for the 1D spin-orbital model (3) of  $L = 8$  sites at  $\Delta = 0$  and  $y = -1/4$ : (a)  $S^{zz}(k)$  and (b)  $T^{zz}(k)$ . Bottom— Spin dimer correlations  $D(r)$  Eq. (5) found at  $\Delta = 0.5$  for decreasing  $1/r$  for clusters of (c)  $L = 12$  and (d)  $L = 16$  sites.

(S/O) phases, I-IV in Fig. 1(a), have  $S_{\text{vN}}^0 = 0$ , i.e., spins and orbitals disentangle in these ground states. If both subsystems display quantum fluctuations,  $|\Psi_0\rangle$  can no longer be written in product form. This occurs for the AS/AO phase III at  $\Delta > 0$ .

Most remarkable is the strongly entangled phase V at  $\Delta = 0$  and  $y < 0$  [Fig. 1(a)]. It occurs near  $x \simeq -\langle \vec{S}_j \cdot \vec{S}_{j+1} \rangle_{\text{AF}} \equiv \ln 2 - 1/4$ , i.e., when the uniform AF spin correlations in phase III are compensated by  $x$ , so that the Hamiltonian Eq. (3) *de facto disappears*. This triggers state V with strong SOE as the only option to gain energy. The analysis of phase V in terms of the longitudinal equal-time spin and orbital structure factors with  $O = S (T)$ ,

$$O^{zz}(k) = \frac{1}{L^2} \sum_{m,n=1}^L e^{-ik(m-n)} \langle O_m^z O_n^z \rangle, \quad (4)$$

reveals  $S^{zz}(k) \propto (1 - \cos k)$  [Fig. 2(a)]. This is a manifestation that further neighbor spin correlations vanish, moreover we find a quadrupling in the orbital sector [Fig. 2(b)]. The spin correlations indicate either a short-range spin liquid or a translational invariant dimer state.

The *hidden spin-dimer order* [47] can be detected by the

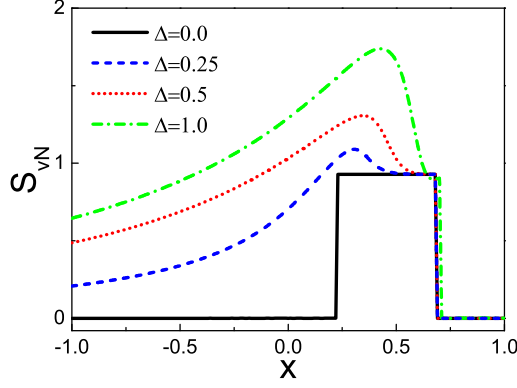


FIG. 3. (color online). Spin-orbital entanglement entropy  $S_{vN}^0$  in the ground state of the spin-orbital model (3) as a function of  $x$  for various  $\Delta$ . Solid line for  $\Delta = 0$  stands for the  $k = 0$  ground state in the limit of  $\Delta \rightarrow 0$  [56]. Parameters:  $y = -0.5$  and  $L = 8$ .

four-spin correlator (we use periodic boundary conditions),

$$D(r) = \frac{1}{L} \sum_{j=1}^L \left[ \left\langle (\vec{S}_j \cdot \vec{S}_{j+1})(\vec{S}_{j+r} \cdot \vec{S}_{j+1+r}) \right\rangle - \left\langle \vec{S}_j \cdot \vec{S}_{j+1} \right\rangle^2 \right]. \quad (5)$$

At  $\Delta = 0$  we find  $|D(r)|$  with long-range dimer correlations in phase V, but not in III. Phase III is a state with alternating ( $k = \pi$ ) spin (orbital) correlations in the range  $x < 0.17$  [Figs. 2(a,b)]. Interestingly for  $\Delta > 0$  the dimer spin correlations  $|D(r)|$  are not only present in V but also appear in phase III, moreover a phase VI emerges, complementary to V, with interchanged role of spins and orbitals [48], see Fig. 1(b). From the size dependence of  $|D(r)|$  in Figs. 2(c,d) we conclude that the dimer correlations are long-ranged at  $\Delta = 0.5$  in phase V, but also in III, as seen from the data for  $x \in [0.0, 0.4)$ , where they coexist with the AS correlations.

These results suggest that the ground state V is formed by spin-singlet product states  $|\Phi_1^D\rangle = [1, 2][3, 4] \cdots [N-1, N]$  and  $|\Phi_2^D\rangle = [2, 3][4, 5] \cdots [N, 1]$ , where  $[l, l+1] = (|\uparrow\downarrow\rangle - |\downarrow\uparrow\rangle)/\sqrt{2}$  denotes a spin singlet. The four-fold ( $k = \pi/2$ ) periodicity of orbital correlations is consistent with orbital states:  $|\Psi_1^z\rangle = |++--\cdots--\rangle$ ,  $|\Psi_2^z\rangle = |-+-+\cdots+-\rangle$ ,  $|\Psi_3^z\rangle = |--++\cdots++\rangle$ , and  $|\Psi_4^z\rangle = |+- - + \cdots - +\rangle$ . The decoupling of singlets is complete for  $y = -1/4$  and  $\Delta = 0$ , where  $(++)$  and  $(--)$  bonds yield vanishing coupling in Eq. (3), and the phase boundaries of region V are  $x_{III,V}^c = 3/4 + 2\langle \vec{S}_j \cdot \vec{S}_{j+1} \rangle_{AF} \simeq 0.136$  and  $x_{V,II}^c = 3/4$ , in the thermodynamic limit; moreover we find perfect long-range order of spin singlets, i.e.,  $D(r) = (3/8)^2(-1)^r$ .

The dimerized spin-singlet state at  $\Delta = 0$  has the same spin structure as the Majumdar-Ghosh (MG) state [49], however its origin is different. While the MG state in a  $J_1$ - $J_2$  Heisenberg AF chain results from frustration (at  $J_2 = J_1/2$ ), here the spin singlets are induced by the SOE. At  $\Delta = 0$  the only phase with finite SOE  $S_{vN}^0 = 1$  is phase V, see Fig. 3. In

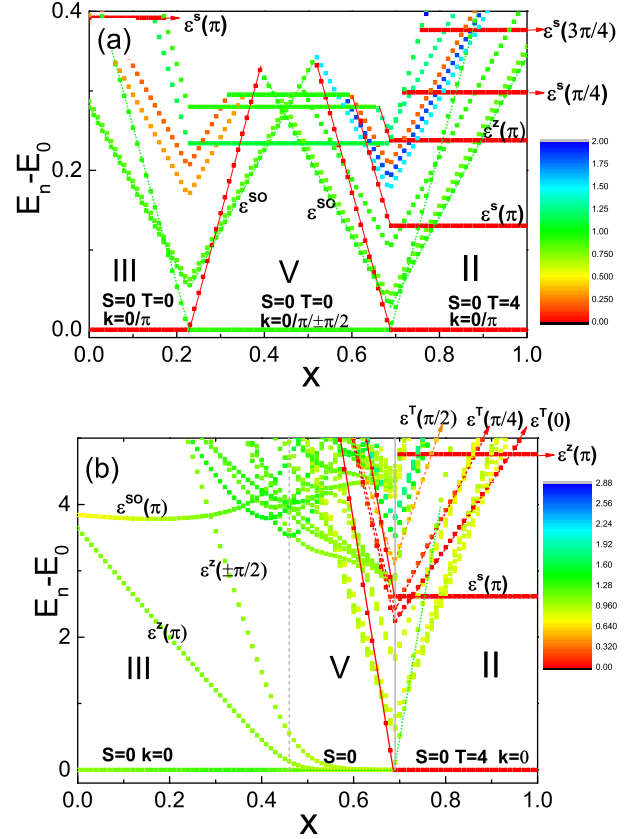


FIG. 4. (color). vNE-spectrum of lowest energies  $E_n(x)$  (relative to the ground state energy  $E_0(x)$ ) versus  $x$  with colors representing the size of the vNE of individual states. Data is shown for  $y = -0.5$ ,  $L = 8$  and: (a)  $\Delta = 0$ , and (b)  $\Delta = 0.5$ . Here  $\varepsilon^S(k)$  [ $\varepsilon^T(k)$ ] denotes spin (orbital) excitation,  $\varepsilon^z(k)$  corresponds to an elementary excitation having the same  $S$  and  $T$  as the ground state, and  $\varepsilon^{SO}(k)$  stands for the spin excitation under simultaneous flipping of orbitals.

contrast, for  $\Delta > 0$  one finds finite EE also in phase III, when the original product ground state changes into a more complex superposition of states and joint spin-orbital fluctuations [8] appear. These correlations control the SOE and give equivalent information to  $S_{vN}^0$ , see the Supplemental Material [50]. Furthermore, EE increases with  $x$  towards phase V where it is further amplified and exceeds  $S_{vN}^0 = 1$ . The related softening of orbital order will be discussed below. Interestingly we find a one-to-one correspondence of finite EE and long-range order in the spin dimer correlations  $|D(r)|$ .

The superstructure of phase V emerges from the interplay of spin and orbitals, where orbitals modulate the interaction of spins in Eq. (3), and *vice versa*. It is important to distinguish this from the Peierls effect, where the coupling to the lattice is an essential mechanism. The orbital Peierls effect observed in vanadates [10, 11] or the orbital-selective Peierls transition [51] fall into the former category, yet, as they involve orbital singlets — they are distinct from the case discussed here.

Figure 3 stimulates a question about the origin of the EE

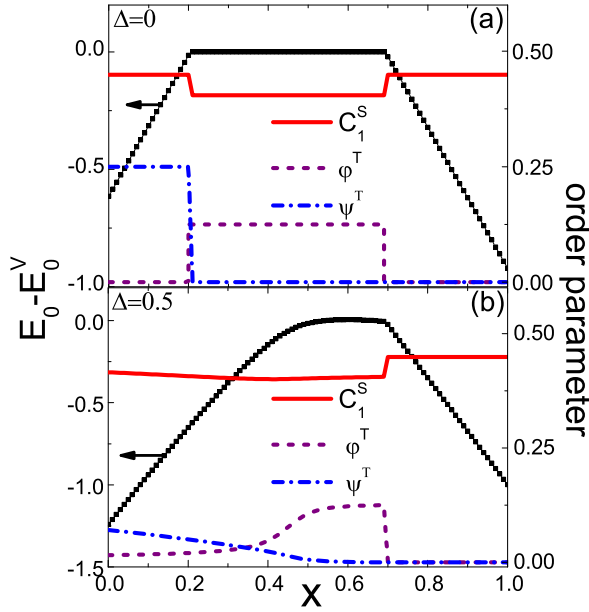


FIG. 5. (color online). Ground state energy relative to phase V,  $E_0 - E_0^V$  (dots), orbital order parameters (dashed),  $\psi^T = [T^{zz}(\pi)]^{\frac{1}{2}}$ ,  $\varphi^T = [T^{zz}(\pi/2)]^{\frac{1}{2}}$ , and spin correlations  $C_1^S = -\langle \vec{S}_1 \cdot \vec{S}_2 \rangle$  (solid line), for phases III, V and II (from left to right), for: (a)  $\Delta = 0.0$  and (b)  $\Delta = 0.5$ . Parameters:  $y = -0.5$  and  $L = 12$ .

changes at phase transitions. It can be resolved by exploring the vNE spectral function defined in Eq. (2) and shown in Figs. 4(a) and 4(b) for  $\Delta = 0$  and  $0.5$ , where colors encode the vNE of states. The excitation energies,  $\omega_n(x) = E_n(x) - E_0(x)$ , include: (i) elementary excitations of the respective ground state, and (ii) many-body excited states that are relevant for the phase transition(s) and may become ground states or elementary excitations in neighboring phases.

The AS/FO ground state of phase II in Fig. 4(a) is an AS singlet ( $S = 0$ ) with a maximal orbital quantum number,  $T = L/2 = 4$ , and a twofold ( $k = 0, \pi$ ) degeneracy at  $\Delta = 0$ . The spin excitation spectrum appears as horizontal (red) lines and consists of gapless spin  $S = 1$  excitation. The low-lying excitations of the Bethe-Ansatz-solvable AF Heisenberg chain form a two-spinon ( $s-\bar{s}$ ) continuum, whose lower bound is given by  $\varepsilon(k) = \pi |\sin k|/2$  in the thermodynamic limit [52]. For the  $L = 8$  chain the spectrum is discrete with a  $\Delta k = \pi/4$  spacing, and it is known that the triplet excitations,  $\varepsilon^S(\pi)$ , will scale to zero as  $1/L$  [53–55]. Red lines in phase II with finite slope are orbital excitations. The  $x$ -dependence is due to the spin part of  $\mathcal{H}$ , which determines both the orbital energy scale and the dispersion  $J_T \equiv (x + \langle \vec{S}_j \cdot \vec{S}_{j+1} \rangle_{AF})(1 - \Delta \cos k)$ . This energy changes with  $x$  and at finite  $\Delta$  with momentum  $k$ , see Fig. 4(b). While the orbitons are gapped, the low-lying excitations are either magnons or  $x$ -dependent spin-orbital excitations. It is remarkable that the latter are entangled in general, although the ground state II is disentangled.

With decreasing  $x$  a first-order phase transition from II to V occurs by level crossing of disentangled (red) and entangled

(green) ground states. The spin-singlet ( $S = 0$ ) ground state of phase V at  $\Delta = 0$  has degeneracy 4, and its components are labeled by the momenta  $k = 0, \pm\pi/2, \pi$  [56]. This is reflected by finite  $\varphi^T$  order parameter in Fig. 5(a). In the spin-dimer phase a gap opens in the spectrum of elementary spin excitations [57, 58]. The one-magnon triplet gap  $\Delta_S(\delta) \propto \delta^{3/4}$  depends on  $y$  via the dimerization parameter  $\delta \equiv 1/|4y|$ . In phase V even the pure magnetic excitations are entangled [see horizontal green lines in Fig. 4(a)]. The lowest excitations in the vicinity of the phase transitions have orbital character. From finite EE in Fig. 4(a) one recognizes that these states are inseparable spin-orbital excitations.

The phase transition from the dimer phase V to the AS ( $S = 0$ ) phase III appears singular in the sense that it is first order at  $\Delta = 0$  and continuous otherwise [Figs. 4(a,b)]. The peculiar feature of the AS/AO phase III also manifests itself in a twofold degeneracy and zero SOE at  $\Delta = 0$  and the non-degenerate ground state and finite SOE at finite  $\Delta$ . The entanglement has two sources, namely the interplay of quantum fluctuations in the spin and orbital sectors and the dimerization order which coexists in phase III at finite  $\Delta$ . The latter is the origin of the nondegenerate ground state as it yields a coupling to the  $\varepsilon^{SO}(\pi)$  excitation (nearly horizontal in  $x$ ), and the emergence of the spin-dimer correlations  $D(r)$  leads to a faster decay of the AF spin correlations in III, see the Supplemental Material [50]. The orbital order parameters  $\psi^T$  and  $\varphi^T$  compete in phases III and V, see Fig. 5(b), near the phase boundary in Fig. 1(b). This also explains why the transition from phase V to III is smooth at finite  $\Delta$  in terms of both the vNE (Fig. 3) and the nearest-neighbor spin correlations  $C_1^S$ .

Summarizing, we have studied the quantum phases and the SOE of the 1D ferromagnetic spin-orbital  $SU(2) \otimes XXZ$  model by means of the Lanczos method. We have discovered a previously unknown translational invariant phase V with long-range spin singlet order and four-fold periodicity in the orbital sector. Its mechanism is distinct from the dimer phases found in the 1D antiferromagnetic spin-orbital model near the  $SU(4)$  symmetric point [39]. Both III-V and II-V phase transitions arise from the SOE in the case of Ising orbital interactions. When the orbital interactions change from Ising to anisotropic  $XXZ$ -type, the entanglement in phase III develops, where antiferromagnetic spin correlations and long-range spin dimer order coexist, changing the quantum phase transition from first-order to continuous.

We have shown that the von Neumann entropy spectral function  $S_{vN}(\omega)$  (2) is a valuable tool that captures the SOE of excitations and explains the origin of the entanglement entropy change in a phase transition. From the perspective of spin-orbital entanglement we encounter (i) first-order transitions between disentangled (II) and entangled (V) phases, (ii) a continuous transition involving two competing order parameters between two entangled phases, III and V, and (iii) trivial first-order transitions between two disentangled phases. Case (ii) goes beyond the commonly accepted paradigm of a single order parameter to characterize a quantum phase — it is an experimental challenge to find such a situation.

*Acknowledgments*— We thank Bruce Normand for insightful discussions. We acknowledge support by the Natural Science Foundation of Jiangsu Province of China under Grant No. BK20141190 and the NSFC under Grant No. 11474211 (W.-L.Y.), as well as by the Polish National Science Center (NCN) under Project No. 2012/04/A/ST3/00331 (A.M.O.).

## SUPPLEMENTAL MATERIAL

In this Supplemental Material we provide complementary information about spin and spin-orbital correlations in the one-dimensional (1D) spin-orbital chain with anisotropic  $XXZ$  orbital interactions. In the first Section A we present additional numerical evidence which demonstrates the spin-orbital entanglement by direct calculation of quartic spin-orbital correlation functions. In the second Section B we discuss the effect of the long-range spin-singlet order that emerges in phase III, that is the antiferro spin (AS) and alternating orbital (AO) phase, on the intrinsic antiferromagnetic (AF) spin correlations.

### A. Spin-orbital entanglement and correlation functions

The description of spin-orbital entanglement in terms of the von Neumann entropy, as discussed in the main text, is a very convenient and popular measure of entanglement. But it is also a highly abstract measure. To capture its meaning, one has to refer to mathematical intuition, namely to the fact that any product state has zero von Neumann entropy. That is, an entangled state is a state that cannot be written as a single product. A more physical measure are obviously spin-orbital correlation functions relative to their mean-field value. Such correlation functions vanish for product states where mean-field factorization of the relevant product is exact, i.e., spins and orbitals are disentangled.

To detect spin-orbital entanglement in the ground state we evaluate here the joint spin-orbital bond correlation function  $C_1$  for the  $SU(2) \otimes XXZ$  model (3), defined as follows for a nearest neighbor bond  $\langle i, i+1 \rangle$  in the ring of length  $L$  [8]:

$$C_1 \equiv \frac{1}{L} \sum_{i=1}^L \left\{ \left\langle \left( \vec{S}_i \cdot \vec{S}_{i+1} \right) \left( \vec{T}_i \cdot \vec{T}_{i+1} \right) \right\rangle - \left\langle \vec{S}_i \cdot \vec{S}_{i+1} \right\rangle \left\langle \vec{T}_i \cdot \vec{T}_{i+1} \right\rangle \right\}, \quad (6)$$

and we compare with the conventional intersite spin- and orbital correlation functions:

$$S_r \equiv \frac{1}{L} \sum_{i=1}^L \left\langle \vec{S}_i \cdot \vec{S}_{i+r} \right\rangle, \quad (7)$$

$$T_r \equiv \frac{1}{L} \sum_{i=1}^L \left\langle \vec{T}_i \cdot \vec{T}_{i+r} \right\rangle. \quad (8)$$

The above general expressions imply averaging over the exact (translational invariant) ground state found from Lanczos

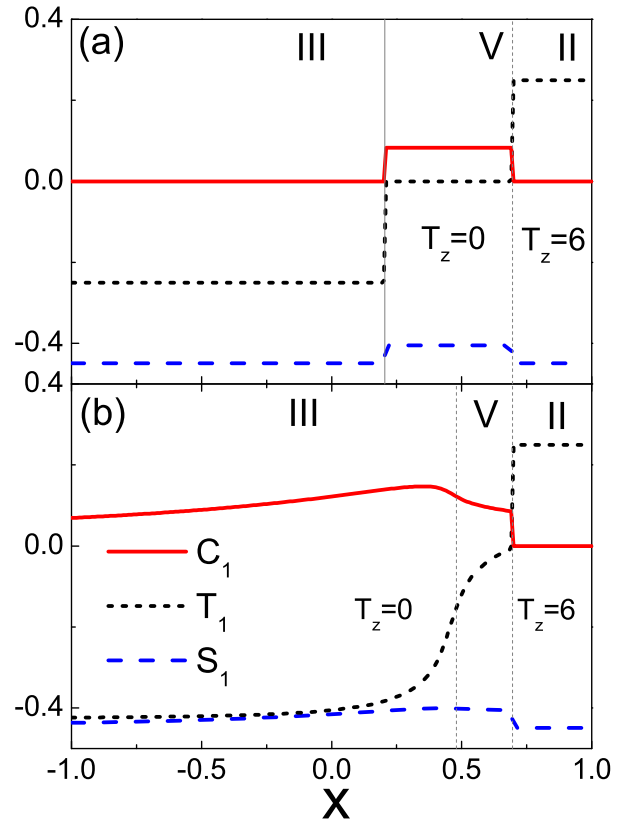


FIG. 6. Nearest neighbor spin  $S_1$  (7), orbital  $T_1$  (8), and joint spin-orbital  $C_1$  (6) correlations as obtained for a spin-orbital ring (3) with  $L = 12$  sites and  $y = -0.5$ , as functions of  $x$  for: (a)  $\Delta = 0$ , and (b)  $\Delta = 0.5$ . The III-V phase boundary (dotted vertical line) in (b) has been determined by the maximum of the fidelity susceptibility [46].

diagonalization of a ring. While  $S_r$  and  $T_r$  correlations indicate the tendency towards particular spin and orbital order,  $C_1$  quantifies the spin-orbital entanglement — if  $C_1 \neq 0$  spin and orbital degrees of freedom are entangled and the mean-field decoupling in Eq. (3) cannot be applied as it generates uncontrollable errors.

Figures 6(a) and 6(b) show the nearest-neighbor correlation functions  $S_1$ ,  $T_1$  and  $C_1$  at  $y = -0.5$ , for  $\Delta = 0$  and  $\Delta = 0.5$ , respectively, as functions of  $x$ . The nearest neighbor spin correlation function  $S_1$  is AF (negative) in all phases shown III, V and II, while  $T_1$  is AO (negative) in phase III and ferro-orbital (positive) in phase II. Finite  $\Delta = 0.5$  triggers orbital fluctuations which lower  $T_1$  below the classical value of 0.25 found at  $\Delta = 0$ . In the intermediate spin dimer phase  $T_1$  is negative for all  $\Delta > 0$ , while it is zero for  $\Delta = 0$ .

It is evident that  $C_1$  is positive in phase V at  $\Delta = 0$  [Fig. 6(a)] and in phases III and V at  $\Delta = 0.5$  [Fig. 6(b)]. Note that positive  $C_1$  occurs in the present spin-orbital chain with  $J < 0$ , while  $C_1$  is negative when  $J > 0$  [36]. In phase II  $C_1$  is always zero as it can be then written as a product ground state. The same is true for phase III at  $\Delta = 0$ . The reader

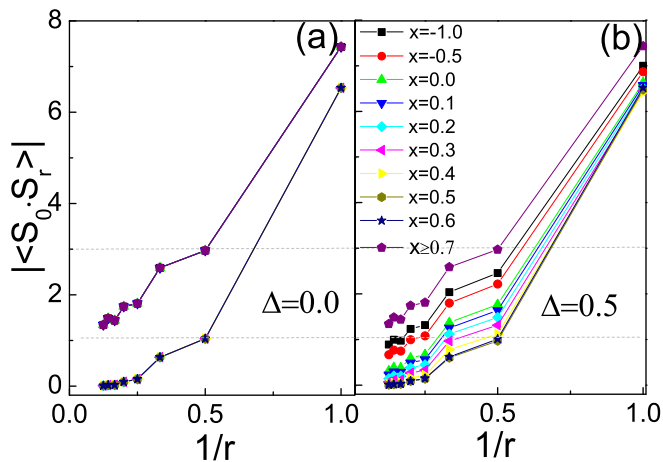


FIG. 7. Spin-correlations  $S_r$  Eq. (7) versus the inverse distance  $1/r$  as obtained for a spin-orbital ring (3) with  $L = 16$  sites, for: (a)  $\Delta = 0$ , and (b)  $\Delta = 0.5$ , respectively. Parameter:  $y = -0.5$ .

recognizes the completely analogous behavior of  $C_1$  as function of  $x$  to that of the von Neumann entropy in Fig. 3 (in the paper), which also displays a broad maximum in the vicinity of the III-V phase transition at  $\Delta = 0.5$ , and a step-like structure in phase V at  $\Delta = 0$ . Thus we conclude here that the von Neumann entropy yields a faithful measure of spin-orbital entanglement that is qualitatively *equivalent* to the more direct entanglement measure via the spin-orbital correlation function  $C_1$  [8].

### B. Spin correlations in phase III

Next we explore the competition of the AF spin correlations of the spin-orbital chain in phase III and the spin-singlet dimer correlations that coexist at finite  $\Delta$ , as we found in our work. For  $\Delta = 0$  the spin correlations in phase III are those of an AF Heisenberg spin chain,

$$\langle \vec{S}_i \cdot \vec{S}_{i+r} \rangle \sim (-1)^r \frac{\sqrt{\ln|r|}}{|r|}, \quad (9)$$

which reveal the typical  $1/r$ -power law decay combined with logarithmic corrections that were first predicted by conformal field theory [59, 60] as well as renormalization group methods [61, 62], and subsequently confirmed by numerical density matrix method [63, 64].

In Fig. 7(a) we present our numerical data for the spin-correlation function  $S_r$  Eq. (7) (i.e., for translational invariant ground states) for several values of  $x$ , and for  $\Delta = 0$  and  $y = -0.5$ . In the  $\Delta = 0$  case there are only two distinct types of behavior of  $S_r$ , namely exponential decay in phase V and the power law decay of the 1D Néel spin liquid state, which are the same in phases II and III.

Figure 7(b) displays  $S_r$  at  $\Delta = 0.5$  for different  $x$ -values. Here again the unperturbed AF correlations of the 1D Néel

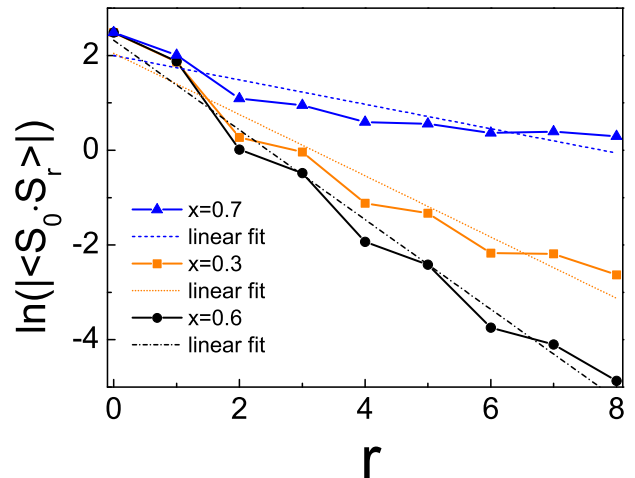


FIG. 8. Logarithm of spin correlations  $S_r$  Eq. (7) for increasing distance  $r$  as obtained for the spin-orbital model Eq. (3) on a ring of  $L = 16$  sites for  $\Delta = 0.5$ ,  $y = -0.5$ , and three values of  $x$ . Exponential decay of  $S_r$  with increasing  $r$  is obtained for phase V ( $x = 0.6$ ).

spin liquid state appear in phase II ( $x \geq 0.7$ ). It is evident that in phase III the AF spin correlations are strongly reduced, due to the competition with the coexisting long-range ordered spin-singlet correlations. The spin singlet order increases with  $x$  in phase III, and as a consequence we observe here that the decay of  $S_r$  becomes stronger as  $x$  approaches the III/V transition.

In Fig. 8 we present a logarithmic plot which highlights for  $\Delta = 0.5$  the different decays of  $S_r$  in the three phases: III, V, and II. We have selected the values for  $x = 0.3, 0.6$  and  $0.7$ , respectively, for greater transparency. The log-plot shows clearly the exponential decay of  $S_r$  in phase V. It also shows that the  $L = 16$  system reveals strong finite size effects in phase II where  $S_r$  has power law decay. Nevertheless it is clear already from the  $L = 16$  data that the AF spin correlations in phase III (here shown for  $x = 0.3$ ) are strongly suppressed and approach the exponential decay of  $S_r$  in phase V ( $x = 0.5$  and  $0.6$ ) when  $x$  approaches the III-V phase boundary from the left.

Summarizing, we find that in phase III the antiferromagnetic spin correlations of the 1D Néel spin liquid state decay much more rapidly as the competing spin-singlet order emerges. This effect is particularly strong near the boundary of phase III to the spin-singlet dimer phase V. Whether in the thermodynamic limit the correlations  $S_r$  also decay exponentially in phase III as in V cannot be decided here, and is beyond the scope of our work.

Moreover we have shown that two measures of entanglement are basically equivalent, namely the direct measure via the (quartic) spin-orbital correlation function  $C_1$  and the von Neumann entropy used in our work.

- 
- [1] K.I. Kugel and D.I. Khomskii, JETP **37**, 725 (1973); Sov. Phys. Usp. **25**, 231 (1982).
- [2] Y. Tokura and N. Nagaosa, Science **288**, 462 (2000).
- [3] A.M. Oleś, G. Khaliullin, P. Horsch, and L.F. Feiner, Phys. Rev. B **72**, 214431 (2005).
- [4] J.-S. Zhou, Y. Ren, J.-Q. Yan, J.F. Mitchell, and J.B. Goodenough, Phys. Rev. Lett. **100**, 046401 (2008).
- [5] P. Corboz, M. Lajkó, A.M. Läuchli, K. Penc, and F. Mila, Phys. Rev. X **2**, 041013 (2012).
- [6] G. Khaliullin and S. Maekawa, Phys. Rev. Lett. **85**, 3950 (2000).
- [7] P. Horsch, A.M. Oleś, L.F. Feiner, and G. Khaliullin, Phys. Rev. Lett. **100**, 167205 (2008).
- [8] A.M. Oleś, P. Horsch, L.F. Feiner, and G. Khaliullin, Phys. Rev. Lett. **96**, 147205 (2006).
- [9] A.M. Oleś, J. Phys.: Condens. Matter **24**, 313201 (2012).
- [10] C. Ulrich, G. Khaliullin, J. Sirker, M. Reehuis, M. Ohl, S. Miyasaka, Y. Tokura, and B. Keimer, Phys. Rev. Lett. **91**, 257202 (2003).
- [11] J. Sirker, A. Herzog, A.M. Oleś, and P. Horsch, Phys. Rev. Lett. **101**, 157204 (2008); A. Herzog, P. Horsch, A.M. Oleś, and J. Sirker, Phys. Rev. B **83**, 245130 (2011).
- [12] L. Amico, R. Fazio, A. Osterloh, and V. Vedral, Rev. Mod. Phys. **80**, 517 (2008).
- [13] H.-Q. Zhou, T. Barthel, J. O. Fjaerestad, and U. Schollwöck, Phys. Rev. A **74**, 050305(R) (2006).
- [14] K. Byczuk, J. Kunes, W. Hofstetter, and D. Vollhardt, Phys. Rev. Lett. **108**, 087004 (2012).
- [15] K. Held and N.J. Mauser, Eur. Phys. J. B **86**, 328 (2013).
- [16] C.N. Veenstra, Z.-H. Zhu, M. Raichle, B.M. Ludbrook, A. Nicolaou, B. Slomski, G. Landolt, S. Kittaka, Y. Maeno, J.H. Dil, I.S. Elfimov, M.W. Haverkort, and A. Damascelli, Phys. Rev. Lett. **112**, 127002 (2014).
- [17] M.Z. Hasan and C.L. Kane, Rev. Mod. Phys. **82**, 3045 (2010).
- [18] G. Jackeli and G. Khaliullin, Phys. Rev. Lett. **102**, 017205 (2009).
- [19] A.V. Gorshkov, M. Hermele, V. Gurarie, C. Xu, P.S. Julianne, J. Ye, P. Zoller, E. Demler, M.D. Lukin, and A.M. Rey, Nature Phys. **6**, 289 (2010).
- [20] S. Mühlbauer, B. Binz, F. Jonietz, C. Pfleiderer, A. Rosch, A. Neubauer, R. Georgii, and P. Böni, Science **323**, 915 (2009).
- [21] R. Lundgren, V. Chua, and G.A. Fiete, Phys. Rev. B **86**, 224422 (2012).
- [22] R. Thomale, D.P. Arovas, and B.A. Bernevig, Phys. Rev. Lett. **105**, 116805 (2010).
- [23] W.-L. You, A.M. Oleś, and P. Horsch, Phys. Rev. B **86**, 094412 (2012).
- [24] H. Li and F.D.M. Haldane, Phys. Rev. Lett. **101**, 010504 (2008).
- [25] F. Pollmann, A.M. Turner, E. Berg, M. Oshikawa, Phys. Rev. B **81**, 064439 (2010).
- [26] V. Alba, M. Haque, and A.M. Läuchli, Phys. Rev. Lett. **108**, 227201 (2012).
- [27] D. Poilblanc, Phys. Rev. Lett. **105**, 077202 (2010).
- [28] L. Fidkowski, Phys. Rev. Lett. **104**, 130502 (2010); N. Regnault and B.A. Bernevig, Phys. Rev. X **1**, 021014 (2011).
- [29] F. Kolley, S. Depenbrock, I.P. McCulloch, U. Schollwöck, and V. Alba, Phys. Rev. B **88**, 144426 (2013).
- [30] R. Lundgren, J. Blair, M. Greiter, A. Läuchli, G.A. Fiete, and R. Thomale, arXiv:1404.7545.
- [31] A. Chandran, V. Khemani, and S.L. Sondhi, Phys. Rev. Lett. **113**, 060501 (2014).
- [32] L.J.P. Ament, M. van Veenendaal, T.P. Devereaux, J.P. Hill, and J. van den Brink, Rev. Mod. Phys. **83**, 705 (2011).
- [33] G. Khaliullin, Prog. Theor. Phys. Suppl. **160**, 155 (2005).
- [34] E. Zhao and W.V. Liu, Phys. Rev. Lett. **100**, 160403 (2008); C. Wu, *ibid.* **100**, 200406 (2008).
- [35] G. Sun, G. Jackeli, L. Santos, and T. Vekua, Phys. Rev. B **86**, 155159 (2012).
- [36] Y.-Q. Li, M. Ma, D.-N. Shi, and F.-C. Zhang, Phys. Rev. Lett. **81**, 3527 (1998); B. Frischmuth, F. Mila, and M. Troyer, *ibid.* **82**, 835 (1999).
- [37] E. Orignac, R. Citro, and N. Andrei, Phys. Rev. B **61**, 11533 (2000).
- [38] Y. Yamashita, N. Shibata, and K. Ueda, J. Phys. Soc. Jpn. **69**, 242 (2000).
- [39] Peng Li and Shun-Qing Shen, Phys. Rev. B **72**, 214439 (2005).
- [40] A.K. Kolezhuk and H.-J. Mikeska, Phys. Rev. Lett. **80**, 2709 (1998).
- [41] A.K. Kolezhuk, H.-J. Mikeska, and U. Schollwöck, Phys. Rev. B **63**, 064418 (2001).
- [42] M.J. Martins and B. Nienhuis, Phys. Rev. Lett. **85**, 4956 (2000).
- [43] B. Kumar, Phys. Rev. B **87**, 195105 (2013).
- [44] W. Brzezicki, J. Dziarmaga, and A.M. Oleś, Phys. Rev. Lett. **112**, 117204 (2014).
- [45] A.M. Belemuk, N.M. Chtchelkatchev, and A.V. Mikheyenkov, Phys. Rev. A **90**, 023625 (2014).
- [46] W.-L. You, Y.-W. Li, and S.-J. Gu, Phys. Rev. E **76**, 022101 (2007).
- [47] Y. Yu, G. Müller, and V.S. Viswanath, Phys. Rev. B **54**, 9242 (1996).
- [48] Phases V and VI were overlooked before at  $\Delta = 1$  [23].
- [49] C.K. Majumdar and D. Ghosh, J. Math. Phys. **10**, 1388 (1969).
- [50] See the Supplemental Material at [http://link.aps.org/...](http://link.aps.org/) for more details on spin-orbital correlations.
- [51] S.V. Streltsov and D.I. Khomskii, Phys. Rev. B **89**, 161112(R) (2014).
- [52] J. des Cloizeaux and J.J. Pearson, Phys. Rev. **128**, 2131 (1962).
- [53] P. Horsch and W. von der Linden, Z. Phys. B **72**, 181 (1988).
- [54] I. Affleck, Rev. Math. Phys. **6**, 887 (1993).
- [55] T. Koma and H. Tasaki, J. Stat. Phys. **76**, 745 (1994).
- [56] At  $\Delta > 0$  this four-fold ground state degeneracy is lifted.
- [57] G. Spronken, B. Fourcade, and Y. Lépine, Phys. Rev. B **33**, 1886 (1986).
- [58] G.S. Uhrig and H.J. Schulz, Phys. Rev. B **54**, R9624 (1996).
- [59] I. Affleck, D. Gepner, H. Schulz, and T. Ziman, J. Phys. A: Math. and Theor. **22**, 511 (1989).
- [60] S. Lukyanov, Nuclear Physics B **522**, 533 (1998).
- [61] T. Giamarchi and H.J. Schulz, Phys. Rev. B **39**, 4620 (1989).
- [62] R.R. Singh, M.E. Fisher, and R. Shankar, Phys. Rev. B **39**, 2562 (1989).
- [63] K.A. Hallberg, P. Horsch, and G. Martínez, Phys. Rev. B **52**, R719 (1995).
- [64] U. Schollwöck, Rev. Mod. Phys. **77**, 259 (2005).